High-Pressure Optical Microspectroscopy Study on Single-Walled Carbon Nanotubes Encapsulating C60

ARTICLE *in* THE JOURNAL OF PHYSICAL CHEMISTRY C · OCTOBER 2013

Impact Factor: 4.77 · DOI: 10.1021/jp405639t

4 AUTHORS, INCLUDING:

Dr. Badawi Anis
Universität Augsburg
12 PUBLICATIONS **60** CITATIONS

SEE PROFILE

THE JOURNAL OF PHYSICAL CHEMISTRY C

Article

pubs.acs.org/JPCC

High-Pressure Optical Microspectroscopy Study on Single-Walled Carbon Nanotubes Encapsulating C_{60}

B. Anis,[†] F. Börrnert,[‡,¶] M. H. Rümmeli,[§,∥,⊥] and C. A. Kuntscher*[,†]

[†]Experimentalphysik 2, Universität Augsburg, D-86159 Augsburg, Germany

[‡]Institute for Solid State Research, IFW Dresden, P.O. Box 270116, D-01171 Dresden, Germany

[§]IBS Center for Integrated Nanostructure Physics, Institute for Basic Science (IBS), Daejon 305-701, Republic of Korea

[∥]Department of Energy Science, Department of Physics, Sungkyunkwan University, Suwon 440-746, Republic of Korea

[⊥]Institute of Complex Materials, IFW Dresden, P.O. Box 270116, D-01171 Dresden, Germany

[¶]Speziallabor Triebenberg, Technische Universität Dresden, 01062 Dresden, Germany

ABSTRACT: The high-pressure behavior of single-walled carbon nanotubes (SWCNTs) filled with C_{60} molecules, so-called C_{60}@SWCNT peapods, has been investigated by optical spectroscopy using nitrogen and argon as pressure transmitting media. Peapods with a high filling ratio were prepared by the sublimation method and characterized by high-resolution transmission electron microscopy. Optical transmission measurements under high pressure were conducted on films of SWCNTs and C_{60}@SWCNT peapods. As with SWCNTs, the absorption bands observed for peapods exhibit a red-shift under pressure. The relative energy shifts of the optical transitions under pressure are higher than those for empty SWCNTs, demonstrating enhanced hybridization and/or symmetry breaking effects. We find an anomaly in the pressure-induced shifts of the optical transitions at $P_{c1} \approx 6.5$ GPa ($P_{c1} \approx 5.5$ GPa) when using nitrogen (argon) as pressure transmitting medium. The anomaly signals the deformation of the nanotube from circular to an oval shape. The value of P_{c1} is in good agreement with theoretical predictions of the pressure-induced deformation for highly filled peapods with similar average diameter. A plateau in the pressure-induced shifts with an onset at $P_{c2} = 12-13$ GPa indicates a saturation of the pressure-induced effects above this critical pressure.

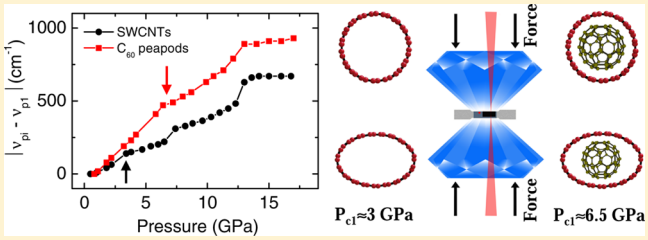

INTRODUCTION

Single-walled carbon nanotubes (SWCNTs) exhibit fascinating mechanical and electronic properties, which can be tuned by doping, strain, or pressure.[1−3] Their robust mechanical properties are due to the strong sp^2 covalent bonds between the carbon atoms network.[4] Theoretical studies[5−7] on the mechanical properties of the carbon nanotubes predict them to be very strong materials, with an axial Young's modulus ≥1 TPa. However, the carbon nanotubes bulk crystals behave as a soft material because they are bound by weak van der Waals forces.[8] Investigations propose that, at a critical pressure, a modification of the nanotubes' cross section from circular to oval, elliptical, or a collapse at high pressure occurs.[9−11]

The mechanical stability of SWCNTs can be affected by filling with molecules or with inner tubes. High-pressure Raman measurements demonstrated that the filling with inner tubes or argon molecules stabilizes the nanotubes; this kind of filling was considered as a case of homogeneous filling.[11−16] In contrast, filling nanotubes with C_{70} and iodine molecules, considered as a case of inhomogeneous filling, leads to the destabilization of the nanotubes.[11,12,15,17,18] This destabilization was explained in terms of the inhomogeneous interaction (noncovalent van der Waals forces) between the nanotube wall and the inner molecules, leading to the tube's mechanical instability at low pressures of ≈1.1−3.5 GPa.[11,12] A recent high-resolution transmission electron microscopy (HRTEM) study by Gorantla et al.[19] proved that the bending of the carbon nanotubes surface enhances the van-der-Walls forces between the tube and the fullerene molecules. The inhomogeneous interaction will be enhanced by the flipping of the C_{70} molecules from the standing to the lying position at ≈1.5 GPa.[11,17]

Earlier high-pressure studies on C_{60}@SWCNT peapods[17,20−23] focused on the issue of polymerization and the rotational dynamics of the C_{60} molecules confined inside SWCNTs. Furthermore, the stability of fullerene peapods against hydrostatic pressure has been mainly addressed by experimental techniques which monitor the vibrational properties, like Raman spectroscopy. To our knowledge, only one work investigated the high-pressure effect on the C_{60} peapods up to 8 GPa using optical spectroscopy, which probes the electronic structure of the peapods.[24] In that work the effect of pressure on the electronic properties of C_{60} peapods was found to be very similar to that in empty SWCNTs. The authors

Received: June 7, 2013
Revised: July 24, 2013

   dx.doi.org/10.1021/jp405639t | J. Phys. Chem. C XXXX, XXX, XXX−XXX

speculated that this similarity is due to the low filling ratio of the peapods.

In general, optical spectroscopy is a powerful technique to characterize the electronic band structure in terms of the energy position and spectral weight of the excited optical transitions. As demonstrated recently, the optical response is capable of monitoring small pressure-induced deformations of the tubular cross-section, since the characteristic van Hove singularities in the density of states in SWCNTs are very sensitive to such deformations.[25,26] Here, we present the results of an optical microspectroscopy study on highly filled C_{60} peapods subjected to high hydrostatic pressure up to ≈18 GPa. The goal of this study was to test the mechanical stability of a carbon nanotube when filled with C_{60} molecules in comparison with empty tubes, via the pressure-induced changes in the optical response.

EXPERIMENTAL SECTION

Chemicals. Bundled SWCNTs were purchased from Carbon Solutions Inc. (Type P2, average diameter 1.4 nm and batch No. 02-444). The P2 SWCNTs were prepared using the arc discharge method. C_{60}-fullerene with purity 99.98% was purchased from Term USA. Triton X-100 (~10% in H_2O) was purchased from Sigma-Aldrich.

Synthesis. To obtain peapods with a high filling ratio, the sublimation method was used.[27] The typical preparation method is described as the following: The caps of the SWCNTs were opened by heating the sample in a furnace at 575 °C (the temperature was increased by 1 °C/min.) for 30 min. Weighted amounts of SWCNTs and C_{60} were degassed under dynamic vacuum (1×10^{-6} mbar) at 200 °C for 24 h. To fill the SWCNTs with the C_{60}, the two materials were sealed in quartz tube under vacuum better than 1×10^{-6} mbar and heated at 750 °C for 5 days continuously. To remove the nonreacted fullerene from the outer surface of the SWCNTs, the peapods were heated at 700 °C under dynamic vacuum for 3 h. Free-standing films from SWCNTs and peapods powder for optical spectroscopy measurements were prepared from Triton X-100 suspension[28] (see Figure 1a–c for illustration).

TEM Characterization. The samples were characterized in different preparation stages with a JEOL JEM-2010F transmission electron microscope retrofitted with two CEOS third-order spherical aberration correctors for the objective lens (CETCOR) and the condenser system (CESCOR). The microscope was operated using an electron acceleration voltage of 80 kV to reduce knock on damage.[29]

Optical Microspectroscopy at High Pressure. Transmittance spectra of the nanotube films were measured at room temperature in the energy range 3500–20 000 cm^{-1} with the resolution 4 cm^{-1} using a Bruker IFS 66v/S Fourier transform infrared spectrometer in combination with an infrared microscope (Bruker IR Scope II) with a 15× Cassegrain objective. For the generation of pressure, a Syassen-Holzapfel type[30] diamond anvil cell (DAC) was used. The culet size of the diamond anvils is 400 μm. Both top and bottom diamond anvil were optically aligned to each other until no observation of Newton rings. By using an electrical discharge drilling machine, a 150 μm hole was drilled in a stainless steel gasket, which served as the sample chamber. For the pressure measurements, a small piece of the free-standing carbon nanotubes film was carefully placed inside the gasket hole with few ruby balls for pressure determination (see Figure 1d). The ruby luminescence technique was used to measure the pressure where the ruby balls are shined by a green leaser of 532 nm wavelength and ≈5 mW power. The laser spot was focused only on the ruby balls for a few seconds to avoid the C_{60} photopolymerization. Liquid nitrogen and argon served as pressure transmitting media. The intensity $I_{sample}(\omega)$ of the radiation transmitted through the sample placed in the DAC and the intensity $I_{ref}(\omega)$ of the radiation transmitted through the pressure transmitting medium in the DAC were measured. From $I_{sample}(\omega)$ and I_{ref} (ω) the transmittance and absorbance spectra were calculated according to $T(\omega) = I_{sample}(\omega)/I_{ref}$ (ω) and $A(\omega) = -\log_{10} T(\omega)$, respectively.

RESULTS AND DISCUSSION

Electron Microscopy. Figure 2 shows the formation of 1D chain peapods from C_{60} inside the SWCNTs. The image indicates also a high filling ratio, which is ≥95%. The high filling ratio of the peapods was confirmed by Raman spectroscopy.[31] The inset of Figure 2 shows that the distance between two adjacent C_{60} molecules is about 1 nm, in good agreement with the earlier published data.[32,33] The high filling ratio in this case could be attributed to the higher temperature used and also the long time of treatment (750 °C and 5 days).

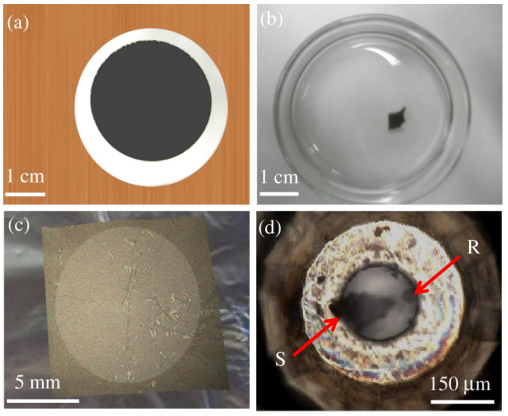

Figure 1. (a) Photograph of the bucky paper. (b) Free-standing carbon nanotubes film floating over acetone solution after dissolution of the cellulose nitrate membrane in the acetone solution. (c) Optical image for the free-standing film over aluminum foil. (d) Optical image of the DAC loaded with carbon nanotubes film (S) and a ruby ball (R) for the pressure determination.

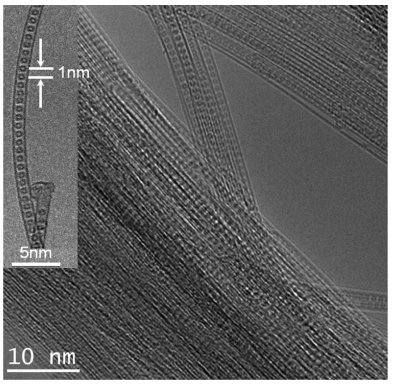

Figure 2. (a) HRTEM image of a bundle of C_{60} peapods after heat treatment at 750 °C for 5 days. The inset shows only one SWCNT filled with C_{60} molecules to confirm the high filling ratio of the peapods.

dx.doi.org/10.1021/jp405639t | J. Phys. Chem. C XXXX, XXX, XXX–XXX

Since the process of increasing the temperature inside the closed quartz tube is an isochoric process, the pressure inside the tube will increase due to the vaporization of more molecules from C_{60} solid.[27] The large number of evaporated molecules arriving at the surface of the SWCNTs and the long heat treatment time are advantageous for the incorporation of the molecules inside the nanotube, leading to a high filling ratio.

Optical Microspectroscopy of SWCNTs and Peapods under Pressure. Figures 3 and 4 show the pressure-dependent absorbance spectra of SWCNTs and peapods, after the background subtraction (see refs 31 and 34 for details), using nitrogen and argon as pressure transmitting medium (PTM), respectively. The insets of Figure 3 show the absorbance spectra of SWCNT and peapods films, respectively, at the lowest pressure (~1 GPa) using nitrogen as PTM together with the total fitting curve and the Lorentz contributions. The insets of Figure 4 depict the absorbance spectra of SWCNT and peapods films, respectively, at the lowest pressure (~0.5−0.8 GPa) using argon as PTM together with the total fitting curve and the Lorentz contributions. The absorption bands S_{ii} and M_{ii} correspond to the ith optical transitions in the semiconducting and metallic SWCNTs, respectively. The optical properties of the free-standing SWCNTs and peapods are explained in detail in our ealier work.[31] It is clear that the absorption bands at the lowest pressure are broadened and the fine-structure due to different tube diameters is smeared out, as compared to the free-standing films (see ref 31). In the further analysis and discussion, only the strong Lorentz contributions will be considered. For both SWCNTs and peapods, we observe only one strong contribution for the S_{11} band and two strong contributions for S_{22} and M_{11} bands, which are marked by $S_{22}(1)$, $S_{22}(2)$ and by $M_{11}(1)$, $M_{11}(2)$, respectively.

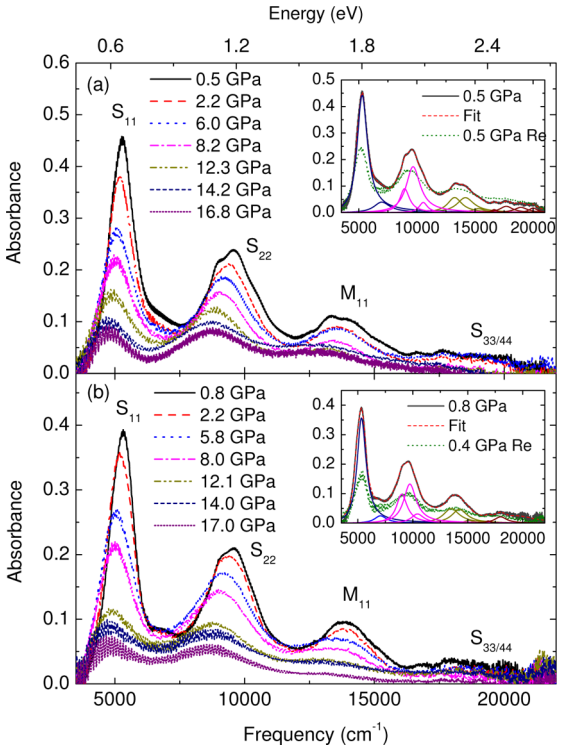

Figure 3. Background-subtracted absorbance spectra of the (a) SWCNT and (b) peapod films as a function of pressure using nitrogen as PTM. The insets in (a) and (b) depict the absorbance spectrum at the lowest pressure during pressure increase together with the various Lorentzian contributions, and the absorbance spectrum at the lowest pressure during pressure release, for the SWCNT and peapod films, respectively.

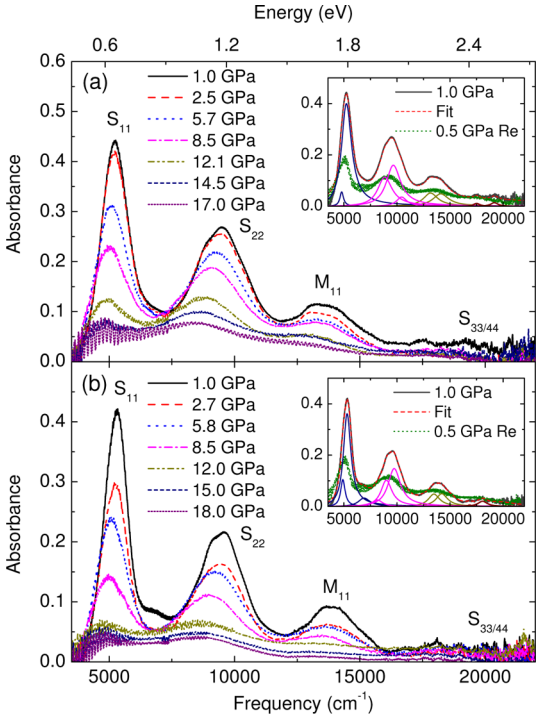

Figure 4. Background-subtracted absorbance spectra of the (a) SWCNT and (b) peapod films as a function of pressure using argon as PTM. The insets in (a) and (b) depict the absorbance spectrum at the lowest pressure during pressure increase together with the various Lorentzian contributions, and the absorbance spectrum at the lowest pressure during pressure release, for the SWCNT and peapod films, respectively.

One notices a red-shift of all the absorption bands for both SWCNT and peapods films under pressure application, with a linear behavior in the low-pressure regime (see Figures 3 and 4). This red-shift is consistent with earlier observations[25,26] and is ascribed to $\sigma^*-\pi^*$ hybridization and/or symmetry breaking.[28,35,36] A detailed comparison between the experimentally observed red-shift and theoretical predictions is given in ref 25. Besides the red-shift, the absorption bands broaden and lose spectral weight with increasing pressure. For nitrogen as PTM, all optical transitions S_{11}, S_{22}, and M_{11} are resolvable up to the highest applied pressure (see Figure 3). In comparison, for argon as PTM, all optical transitions are resolvable up to ≈12 GPa only. Above 12 GPa, the optical transitions become very broad, in particular the M_{11} transition (see Figure 4).

For a quantitative comparison of the pressure-induced red-shifts of the absorption bands, we plot in Figures 5 and 6 the relative energy shifts of the Lorentz contributions as a function of applied pressure. For the SWCNT film under pressure and using nitrogen as PTM (see Figure 5a), two anomalies in the relative pressure-induced shifts are observed at $P_{c1} \approx 3$ GPa and $P_{c2} \approx 7$ GPa. As criteria for the values of the critical pressures, we use (i) the second derivative of the evolution of E_{ii} with pressure and (ii) the deviation from the linear behavior. Above P_{c1}, the relative shifts can be described by fourth order polynomials. The shaded gray areas in Figure 5a correspond to

dx.doi.org/10.1021/jp405639t | J. Phys. Chem. C XXXX, XXX, XXX−XXX

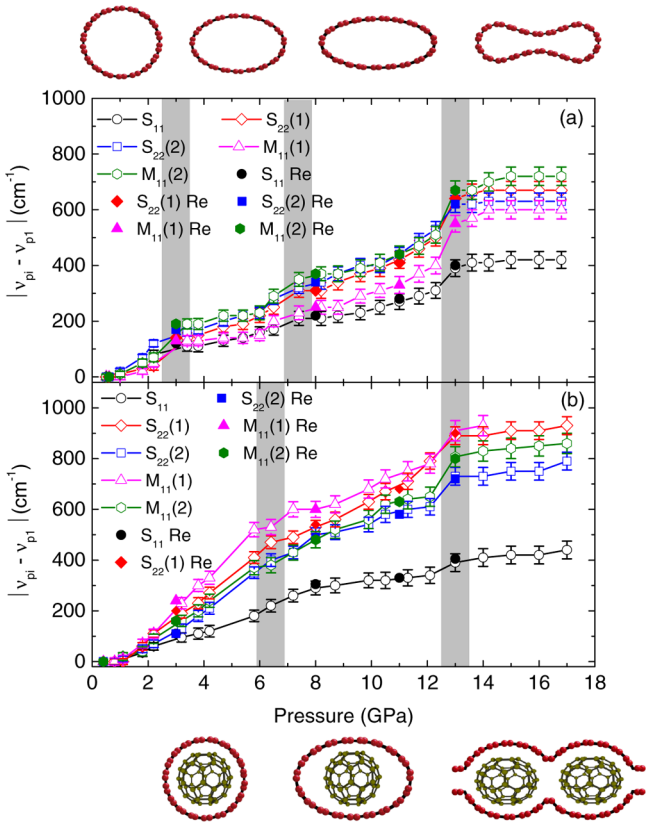

Figure 5. Relative energy shift of the optical transitions as a function of pressure for (a) SWCNT and (b) peapod films using nitrogen as PTM. The shift was calculated as the difference between the absorption frequency of the contribution ν_{pi} at a pressure pi, and the absorption frequency ν_{p1} at the lowest pressure value $p1$. All the contributions during pressure release are marked as S_{ii} (Re) and M_{ii} (Re) for both semiconducting and metallic tubes, respectively. The shaded, gray areas mark the critical pressures regions as discussed in the text. The proposed deformation of the cross sections for SWCNTs and peapods in the different pressure ranges is illustrated.

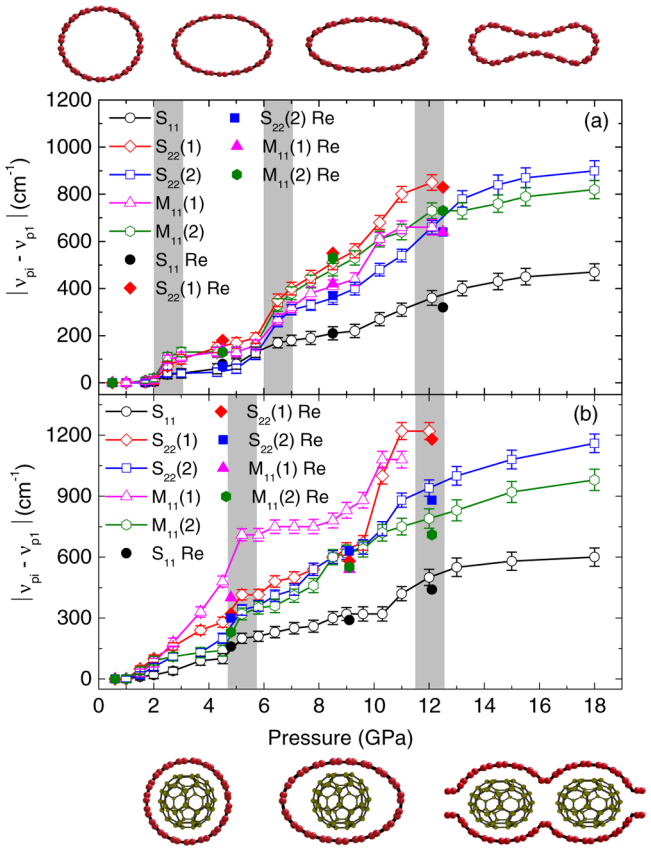

Figure 6. Relative energy shift of the optical transitions as a function of pressure for (a) SWCNT and (b) peapod films using argon as PTM. The shift was calculated as the difference between the absorption frequency of the contribution ν_{pi} at a pressure pi, and the absorption frequency ν_{p1} at the lowest pressure value $p1$. All the contributions during pressure release are marked as S_{ii} (Re) and M_{ii} (Re) for both semiconducting and metallic tubes, respectively. The shaded, gray areas mark the critical pressures regions as discussed in the text. The proposed deformation of the cross sections for SWCNTs and peapods in the different pressure ranges is illustrated.

the pressure regimes in which the anomalies are observed, with an error bar of ±0.5 GPa. According to earlier results and theoretical predictions,[25,37−45] we interpret the anomaly at P_{c1} in terms of a structural phase transition, where the tube is deformed from a circular to an oval shape. Above P_{c2}, a more drastic change in the cross section from oval to race-track or peanut-type shape occurs.[10,11,34] With further pressure increasing above P_{c2}, a steep increase in the relative pressure-induced shifts is found, followed by a plateau with an onset at $P_{c3} \approx 13$ GPa. This plateau indicates a saturation of the pressure-induced deformation and hybridization effects above P_{c3}. According to recent pressure investigations on SWCNTs with an average tube diameter of 1.35 nm, the transition pressure for the collapse of the tubes amounts to ∼14 GPa.[11,12] Accordingly, we interpret the rapid increase in the shifts above ∼11 GPa in terms of the onset of the collapse, which is completed at $P_{c3} \approx 13$ GPa, that is, at the onset of the plateau. The proposed sequence of structural deformations in SWCNTs is illustrated on top of Figure 5.

Figure 6a depicts the relative pressure-induced energy shifts of the optical transitions in SWCNTs using argon as PTM. Compared to the nitrogen data (see Figure 5a), the anomalies in the pressure-induced shifts are lowered to $P_{c1} \approx 2.5$ GPa, $P_{c2} \approx 6.5$ GPa, and $P_{c3} \approx 12$ GPa. For determining the critical pressure values, the above-mentioned criteria have been used. Above P_{c3}, the absorption bands S_{11}, S_{22}, and M_{11} become very broad, and each band can be fitted with one Lorentzian contribution only. Also the relative energy shifts are larger than the corresponding shifts for nitrogen as PTM. The broadening of the absorption bands and the lower critical pressure values can be explained by the lower hydrostaticity level of argon compared to nitrogen as PTM.[46] Furthermore, the onset of the collapse, indicated by the steep increase in the pressure-induced shifts, is more pronounced and happens at a lower pressure in the case of argon as PTM. The proposed sequence of structural deformations in SWCNTs using argon as PTM is illustrated on top of Figure 6.

To clarify the effect of the C_{60} molecules filling on the mechanical stability of the SWCNTs, we plot in Figure 5b the relative pressure-induced shifts of the optical transitions for the C_{60} peapods, using nitrogen as PTM. First, one notices two anomalies in the pressure-induced shifts, namely, at $P_{c1} \approx 6.5$ GPa and $P_{c2} \approx 13$ GPa, followed by a plateau. The critical pressure values have been determined according to the same criteria as for the SWCNTs. Above P_{c1}, the relative shifts can be described by fourth order polynomials. According to an earlier high-pressure X-ray study[21] on C_{60}-peapods, we interpret the

dx.doi.org/10.1021/jp405639t | J. Phys. Chem. C XXXX, XXX, XXX−XXX

anomaly at $P_{c1} \approx 6.5$ GPa in terms of a deformation of the tubes' cross section from circular to oval. Above $P_{c1} \approx 6.5$ GPa, a more drastic ovalization of the tubes is expected. Hereby, the flat or peanut structure is excluded due to steric reasons.[11] It is known that intercalated C_{60} fullerene molecules still have a high bulk modulus and can be considered as nondeformable molecules.[47] For that reason, C_{60}-peapods at high pressure may be transformed to the oval rather than the flat shape.[11] The plateau with the onset at $P_{c2} \approx 13$ GPa indicates a saturation of the pressure-induced deformation and hybridization above this pressure, associated with a collapse. Similar like in the SWCNTs, the collapse starts a few GPa below P_{c2} indicated by the rapid increase in the pressure-induced shifts and is complete at P_{c2}. The proposed sequence of structural deformations in C_{60} peapods is illustrated on the bottom of Figure 5.

In general, we note that the relative energy shifts of the optical transitions for peapods are quite large compared to the empty SWCNTs (see Figure 5a). This finding could be explained as follows: It was observed that with increasing pressure the center-to-center distance between the fullerene molecules inside C_{60} peapods decreases from 0.956 nm at the lowest pressure to 0.855 nm at 10 GPa,[20] forming a closely packed chain inside the nanotube cavity.[23,48] Also, the C_{60} molecules are known to be very hard molecules with a high bulk modulus.[47] The symmetry breaking and hybridization effects in the nanotubes might therefore be enhanced in pressurized peapods, leading to larger pressure-induced shifts of the optical transitions.

Compared to the empty SWCNTs (see Figure 5a), the first structural anomaly in peapods is shifted from ≈3 to ≈6.5 GPa, which signals the stabilization of the nanotubes outer walls by the inner fullerene molecules. This finding is in contrast to earlier Raman studies on SWCNTs filled with C_{70} and iodine,[11,12,17,18] where an anomaly in the radial breathing modes was observed at ∼2−3 GPa for various pressure transmitting media, as observed in SWCNTs. The Raman studies furthermore found a frequency downshift of the tangential optical phonon mode, which was attributed the flipping of the orientation of the C_{70} molecules at low pressure, which enhances the inhomogeneous interactions between the fullerene molecules and the nanotube, or to the formation of short polyiodine chains inside the SWCNTs under pressure. In our case, such kind of flipping or polymerization is not expected due to the high symmetry of the C_{60} molecules.

Recently, theoretical calculations[49,50] estimated the critical pressure for the buckling of SWCNTs and peapods. The calculations suggested such kind of stabilization in the case of the peapods. For the SWCNTs the critical pressure P_c is defined as

$$P_c = \frac{3N^{\alpha}D}{R^3} - \frac{\gamma}{R} \quad (1)$$

where N is the number of walls and the parameter α describes the bonding between walls, which is $\alpha = 1$ in our case, since $N = 1$. D is the bending stiffness of graphene and was determined to ≈0.21 nN nm,[49] and γ is the surface tension of the nanotubes, $\gamma \approx 0.23$ N m^{1-}.[49] The second term is the pressure imposed by the surrounding tubes and the pressure medium, which is significant only at the nanoscale. In our case $N = 1$, $R = 0.7$ nm, and $D = 0.21$ nN nm, so the expected deformation pressure is ≈1.8 GPa (neglecting the effect of the surrounding tubes and the PTM). This critical pressure is slightly lower than typical values from earlier theoretical predictions and experimental results.[25,26,34,39−41,51]

For peapods, the critical pressure P_c is calculated according to

$$P_c = \frac{\pi^2 N^{\alpha} D}{R^3} f^2 - \frac{\gamma}{R} \quad (2)$$

where f is the filling ratio of the nanotubes. In our case, the filling ratio f is close to 1, and therefore, the expected critical pressure P_c for the peapods is 6.0 GPa (neglecting the effect of the surrounding tubes and the PTM). This value is very close to our experimental value $P_{c2} \approx 6.5$ GPa for nitrogen as PTM.

Figure 6b shows the relative pressure-induced energy shifts of the optical transitions for C_{60} peapods using argon as PTM. Compared to the nitrogen data (Figure 5b), the anomalies in the pressure-induced shifts occur at lower pressures, $P_{c1} \approx 5.5$ GPa and $P_{c2} \approx 12$ GPa. Above P_{c2}, all the optical transitions S_{11}, S_{22}, and M_{11} become very broad and can be fitted with one Lorentzian contribution. Also the relative energy shifts are larger than the corresponding shifts for nitrogen as PTM. Like for SWCNTs, the broadening of the absorption bands and the higher critical pressure values are due to the lower hydrostaticity level of argon compared to nitrogen.[46] The onset of the collapse is clearly indicated by the rapid increase of the pressure-induced shifts already above 8−10 GPa, well below P_{c2}.

Interestingly, stabilization effects due to nitrogen or argon filling of the SWCNTs and C_{60}@SWCNT peapods can be ruled out based on our data. In conclusion, neither nitrogen nor argon filling of the SWCNTs and the peapods prevents the occurrence of pressure-induced anomalies in the electronic transitions due to tubular deformation, in contradiction to earlier reports.[52]

Finally, we comment on the reversibility of the pressure-induced structural changes. For both SWCNTs and peapods the pressure-induced frequency shifts of the optical transitions are reversible upon pressure release (see Figures 5 and 6). However, one notices a loss in intensity, namely, up to ∼50% to ∼45% of the original absorbance value for SWCNTs and peapods. This is illustrated in the insets of Figures 5 and 6, where the absorbance spectra at the lowest pressure during pressure release are included. The irreversible changes indicate that a fraction of the tubes has been permanently damaged during pressure loading, with a loss of the characteristic features in their density of states.

In conclusion, the mechanical stability of the outer tubes in peapods under hydrostatic pressure has been characterized in terms of the optical transitions. Compared to empty SWCNTs, the relative energy shifts of the optical transitions for C_{60}@SWCNT peapods are large, indicating that the pressure-induced hybridization and the symmetry breaking effects are increased by the filling with fullerene molecules. The anomaly in the pressure-induced shifts of the absorption bands at around $P_{c1} \approx 6.5$ GPa ($P_{c1} \approx 5.5$ GPa) for nitrogen (argon) as PTM is due to the tubular deformation from a circular to an oval shape. The shift of the anomaly from $P_{c1} \approx 3.0$ GPa (2.5 GPa) for SWCNTs to $P_{c1} \approx 6.5$ GPa (5.5 GPa) for C_{60} peapods in case of nitrogen (argon) as PTM signals the stabilization of the nanotubes walls by the encapsulated fullerene molecules. The value of P_{c1} is in good agreement with theoretical predictions for the pressure-induced structural deformation of highly filled peapods with similar average diameters. The pressure-induced alterations of the absorption bands are reversible regarding their frequency position but not completely reversible regarding their

dx.doi.org/10.1021/jp405639t | J. Phys. Chem. C XXXX, XXX, XXX−XXX

intensity, indicating that a fraction of the tubes has been permanently damaged under high pressure load.

AUTHOR INFORMATION

Corresponding Author

*E-mail: christine.kuntscher@physik.uni-augsburg.de. Phone: +49-(0)821 598 3315. Fax: +49-(0)821 598 3411.

Notes

The authors declare no competing financial interest.

ACKNOWLEDGMENTS

We acknowledge financial support by the DFG (KU1432/3-2, RU1540/8-1), the DAAD, and the Egyptian Government. M.H.R. acknowledges the support of the Institute of Basic Science (IBS) Korea.

REFERENCES

(1) San-Miguel, A. Nanomaterials Under High-Pressure. *Chem. Soc. Rev.* **2006**, *35*, 876−889.

(2) Souza Filho, A. G.; Kobayashi, N.; Jiang, J.; Grüneis, A.; Saito, R.; Cronin, S. B.; Mendes Filho, J.; Samsonidze, G. G.; Dresselhaus, G.; Dresselhaus, M. S. Strain-Induced Interference Effects on the Resonance Raman Cross Section of Carbon Nanotubes. *Phys. Rev. Lett.* **2005**, *95*, 217403.

(3) Zang, J.; Treibergs, A.; Han, Y.; Liu, F. Geometric Constant Defining Shape Transitions of Carbon Nanotubes Under Pressure. *Phys. Rev. Lett.* **2004**, *92*, 105501.

(4) Jorio, A.; Dresselhaus, G.; Dresselhaus, M. S. *Carbon Nanotubes: Advanced Topics in the Synthesis, Structure, Properties and Applications*; Springer-Verlag Berlin: Heidelberg, 2008; Vol. *111*.

(5) Krishnan, A.; Dujardin, E.; Ebbesen, T. W.; Yianilos, P. N.; Treacy, M. M. J. Young's Modulus of Single-Walled Nanotubes. *Phys. Rev. B* **1998**, *58*, 14013−14019.

(6) Hernández, E.; Goze, C.; Bernier, P.; Rubio, A. Elastic Properties of C and $B_xC_yN_z$ Composite Nanotubes. *Phys. Rev. Lett.* **1998**, *80*, 4502−4505.

(7) Lu, J. P. Elastic Properties of Carbon Nanotubes and Nanoropes. *Phys. Rev. Lett.* **1997**, *79*, 1297−1300.

(8) Kawasaki, S.; Matsuoka, Y.; Yokomae, T.; Nojima, Y.; Okino, F.; Touhara, H.; Kataura, H. XRD and TEM Study of High Pressure Treated Single-Walled Carbon Nanotubes and C_{60}-Peapods. *Carbon* **2005**, *43*, 37−45.

(9) Lebedkin, S.; Arnold, K.; Kiowski, O.; Hennrich, F.; Kappes, M. M. Raman Study of Individually Dispersed Single-Walled Carbon Nanotubes Under Pressure. *Phys. Rev. B* **2006**, *73*, 094109.

(10) Yao, M.; Wang, Z.; Liu, B.; Zou, Y.; Yu, S.; Lin, W.; Hou, Y.; Pan, S.; Jin, M.; Zou, B.; et al. Raman Signature to Identify the Structural Transition of Single-Wall Carbon Nanotubes Under High Pressure. *Phys. Rev. B* **2008**, *78*, 205411.

(11) Caillier, C.; Machon, D.; San-Miguel, A.; Arenal, R.; Montagnac, G.; Cardon, H.; Kalbac, M.; Zukalova, M.; Kavan, L. Probing High-Pressure Properties of Single-Wall Carbon Nanotubes Through Fullerene Encapsulation. *Phys. Rev. B* **2008**, *77*, 125418.

(12) Aguiar, A. L.; Barros, E. B.; Capaz, R. B.; Souza Filho, A. G.; Freire, P. T. C.; Filho, J. M.; Machon, D.; Caillier, C.; Kim, Y. A.; Muramatsu, H.; et al. Pressure-Induced Collapse in Double-Walled Carbon Nanotubes: Chemical and Mechanical Screening Effects. *J. Phys. Chem. C* **2011**, *115*, 5378−5384.

(13) Pfeiffer, R.; Kuzmany, H.; Kramberger, C.; Schaman, C.; Pichler, T.; Kataura, H.; Achiba, Y.; Kürti, J.; Zólyomi, V. Unusual High Degree of Unperturbed Environment in the Interior of Single-Wall Carbon Nanotubes. *Phys. Rev. Lett.* **2003**, *90*, 225501.

(14) Puech, P.; Hubel, H.; Dunstan, D. J.; Bacsa, R. R.; Laurent, C.; Bacsa, W. S. Discontinuous Tangential Stress in Double Wall Carbon Nanotubes. *Phys. Rev. Lett.* **2004**, *93*, 095506.

(15) San-Miguel, A.; Cailler, C.; Machon, D.; Barros, E.; Aguiar, A.; Filho, A. In *High-Pressure Crystallography*; Boldyreva, E., Dera, P., Eds.; NATO Science for Peace and Security Series B: Physics and Biophysics; Springer: Netherlands, 2010; pp 435−446.

(16) Shanavas, K. V.; Sharma, S. M. Molecular Dynamics Simulations of Phase Transitions in Argon-Filled Single-Walled Carbon Nanotube Bundles Under High Pressure. *Phys. Rev. B* **2009**, *79*, 155425.

(17) Rafailov, P. M.; Thomsen, C.; Kataura, H. Resonance and High-Pressure Raman Studies on Carbon Peapods. *Phys. Rev. B* **2003**, *68*, 193411.

(18) Alvarez, L.; Bantignies, J.-L.; Le Parc, R.; Aznar, R.; Sauvajol, J.-L.; Merlen, A.; Machon, D.; San Miguel, A. High-Pressure Behavior of Polyiodides Confined into Single-Walled Carbon Nanotubes: A Raman Study. *Phys. Rev. B* **2010**, *82*, 205403.

(19) Gorantla, S.; Avdoshenko, S.; Börrnert, F.; Bachmatiuk, A.; Dimitrakopoulou, M.; Schäffel, F.; Schönfelder, R.; Thomas, J.; Gemming, T.; Warner, J. H.; et al. Enhanced $\pi-\pi$ Interactions Between a C_{60} Fullerene and a Buckle Bend on a Double-Walled Carbon Nanotube. *Nano Res.* **2010**, *3*, 92−97.

(20) Kawasaki, S.; Hara, T.; Yokomae, T.; Okino, F.; Touhara, H.; Kataura, H.; Watanuki, T.; Ohishi, Y. Pressure-Polymerization of C_{60} Molecules in a Carbon Nanotube. *Chem. Phys. Lett.* **2006**, *418*, 260−263.

(21) Chorro, M.; Rols, S.; Cambedouzou, J.; Alvarez, L.; Almairac, R.; Sauvajol, J.-L.; Hodeau, J.-L.; Marques, L.; Mezouar, M.; Kataura, H. Structural Properties of Carbon Peapods Under Extreme Conditions Studied Using *in situ* X-Ray Diffraction. *Phys. Rev. B* **2006**, *74*, 205425.

(22) Zou, Y.; Liu, B.; Yao, M.; Hou, Y.; Wang, L.; Yu, S.; Wang, P.; Li, B.; Zou, B.; Cui, T.; et al. Raman Spectroscopy Study of Carbon Nanotube Peapods Excited by Near-IR Laser Under High Pressure. *Phys. Rev. B* **2007**, *76*, 195417.

(23) Zou, Y.; Liu, B.; Wang, L.; Liu, D.; Yu, S.; Wang, P.; Wang, T.; Yao, M.; Li, Q.; Zou, B.; et al. Rotational Dynamics of Confined C_{60} From Near-Infrared Raman Studies Under High Pressure. *Proc. Natl. Acad. Sci. U.S.A.* **2009**, *106*, 22135−22138.

(24) Kuntscher, C. A.; Abouelsayed, A.; Botos; Pekker; Kamarás, K. Pressure Studies on Fullerene Peapods. *Phys. Status Solidi B* **2011**, *248*, 2732−2735.

(25) Thirunavukkuarasu, K.; Hennrich, F.; Kamarás, K.; Kuntscher, C. A. Infrared Spectroscopic Studies on Unoriented Single-Walled Carbon Nanotube Films Under Hydrostatic Pressure. *Phys. Rev. B* **2010**, *81*, 045424.

(26) Kuntscher, C. A.; Abouelsayed, A.; Thirunavukkuarasu, K.; Hennrich, F. Pressure-Induced Phenomena in Single-Walled Carbon Nanotubes: Structural Phase Transitions and the Role of Pressure Transmitting Medium. *Phys. Status Solidi B* **2010**, *247*, 2789−2792.

(27) Smith, B. W.; Russo, R. M.; Chikkannanavar, S. B.; Stercel, F.; Luzzi, D. E. Reproducible Synthesis of C60@SWNT in 90% Yields. *Mater. Res. Soc. Symp. Proc.* **2002**, *706*, Z.313.1.

(28) Wu, Z.; Chen, Z.; Du, X.; Logan, J. M.; Sippel, J.; Nikolou, M.; Kamaras, K.; Reynolds, J. R.; Tanner, D. B.; Hebard, A. F.; et al. Transparent, Conductive Carbon Nanotube Films. *Science* **2004**, *305*, 1273−1276.

(29) Börrnert, F.; Bachmatiuk, A.; Gorantla, S.; Wolf, D.; Lubk, A.; Büchner, B.; Rümmeli, M. Retro-Fitting an Older (S)TEM with Two C_s Aberration Correctors for 80 kV and 60 kV Operation. *J. Microsc.* **2013**, *249*, 87−92.

(30) Huber, G.; Syassen, K.; Holzapfel, W. B. Pressure Dependence of 4 *f* Levels in Europium Pentaphosphate up to 400 kbar. *Phys. Rev. B* **1977**, *15*, 5123−5128.

(31) Anis, B.; Fischer, M.; Schreck, M.; Haubner, K.; Dunsch, L.; Kuntscher, C. A. Synthesis and Characterization of Peapods and DWCNTs. *Phys. Status Solidi B* **2012**, *249*, 2345−2348.

(32) Hirahara, K.; Suenaga, K.; Bandow, S.; Kato, H.; Okazaki, T.; Shinohara, H.; Iijima, S. One-Dimensional Metallofullerene Crystal Generated Inside Single-Walled Carbon Nanotubes. *Phys. Rev. Lett.* **2000**, *85*, 5384−5387.

(33) Hirahara, K.; Bandow, S.; Suenaga, K.; Kato, H.; Okazaki, T.; Shinohara, H.; Iijima, S. Electron Diffraction Study of One-Dimensional Crystals of Fullerenes. *Phys. Rev. B* **2001**, *64*, 115420.

(34) Anis, B.; Haubner, K.; Börrnert, F.; Dunsch, L.; Rümmeli, M. H.; Kuntscher, C. A. Stabilization of Carbon Nanotubes by Filling with Inner Tubes: An Optical Spectroscopy Study on Double-Walled Carbon Nanotubes Under Hydrostatic Pressure. *Phys. Rev. B* **2012**, *86*, 155454.
(35) Charlier, J. C.; Lambin, P.; Ebbesen, T. W. Electronic Properties of Carbon Nanotubes with Polygonized Cross Sections. *Phys. Rev. B* **1996**, *54*, R8377−R8380.
(36) Liu, G.; Wang, X.; Chen, J.; Lu, H. Pressure- and Orientation-Dependent Linear Optical Absorption Spectra of Radially Deformed Single-Walled Carbon Nanotubes. *Phys. Status Solidi B* **2008**, *245*, 689−694.
(37) Capaz, R. B.; Spataru, C. D.; Tangney, P.; Cohen, M. L.; Louie, S. G. Hydrostatic Pressure Effects on the Structural and Electronic Properties of Carbon Nanotubes. *Phys. Status Solidi B* **2004**, *241*, 3352−3359.
(38) Chan, S.-P.; Yim, W.-L.; Gong, X. G.; Liu, Z.-F. Carbon Nanotube Bundles Under High Pressure:Transformation to Low-Symmetry Structures. *Phys. Rev. B* **2003**, *68*, 075404.
(39) Sluiter, M. H. F.; Kawazoe, Y. Phase Diagram of Single-Wall Carbon Nanotube Crystals Under Hydrostatic Pressure. *Phys. Rev. B* **2004**, *69*, 224111.
(40) Elliott, J. A.; Sandler, J. K. W.; Windle, A. H.; Young, R. J.; Shaffer, M. S. P. Collapse of Single-Wall Carbon Nanotubes is Diameter Dependent. *Phys. Rev. Lett.* **2004**, *92*, 095501.
(41) Hasegawa, M.; Nishidate, K. Radial Deformation and Stability of Single-Wall Carbon Nanotubes Under Hydrostatic Pressure. *Phys. Rev. B* **2006**, *74*, 115401.
(42) Venkateswaran, U. D.; Rao, A. M.; Richter, E.; Menon, M.; Rinzler, A.; Smalley, R. E.; Eklund, P. C. Probing the Single-wall carbon Nanotube Bundle: Raman Scattering Under High Pressure. *Phys. Rev. B* **1999**, *59*, 10928−10934.
(43) Peters, M. J.; McNeil, L. E.; Lu, J. P.; Kahn, D. Structural Phase Transition in Carbon Nanotube Bundles Under Pressure. *Phys. Rev. B* **2000**, *61*, 5939−5944.
(44) Sandler, J.; Shaffer, M. S. P.; Windle, A. H.; Halsall, M. P.; Montes-Morán, M. A.; Cooper, C. A.; Young, R. J. Variations in the Raman Peak Shift as a Function of Hydrostatic Pressure for Various Carbon Nanostructures: A Simple Geometric Effect. *Phys. Rev. B* **2003**, *67*, 035417.
(45) Gadagkar, V.; Maiti, P. K.; Lansac, Y.; Jagota, A.; Sood, A. K. Collapse of Double-Walled Carbon Nanotube Bundles Under Hydrostatic Pressure. *Phys. Rev. B* **2006**, *73*, 085402.
(46) Klotz, S.; Chervin, J.-C.; Munsch, P.; Marchand, G. L. Hydrostatic Limits of 11 Pressure Transmitting Media. *J. Phys. D: Appl. Phys.* **2009**, *42*, 075413.
(47) Poloni, R.; Fernandez-Serra, M. V.; Le Floch, S.; De Panfilis, S.; Toulemonde, P.; Machon, D.; Crichton, W.; Pascarelli, S.; San-Miguel, A. Pressure-Induced Deformation of the C_{60} Fullerene in Rb_6C_{60} and Cs_6C_{60}. *Phys. Rev. B* **2008**, *77*, 035429.
(48) Okada, S.; Saito, S.; Oshiyama, A. Energetics and Electronic Structures of Encapsulated C_{60} in a Carbon Nanotube. *Phys. Rev. Lett.* **2001**, *86*, 3835−3838.
(49) Pugno, N. M.; Elliott, J. A. Buckling of Peapods, Fullerenes and Nanotubes. *Phys. E* **2012**, *44*, 944−948.
(50) Pugno, N. M. The Design of Self-Collapsed Super-Strong Nanotube Bundles. *J. Mech. Phys. Solids* **2010**, *58*, 1397−1410.
(51) Abouelsayed, A.; Thirunavukkuarasu, K.; Hennrich, F.; Kuntscher, C. A. Role of the Pressure Transmitting Medium for the Pressure Effects in Single-Walled Carbon Nanotubes. *J. Phys. Chem. C* **2010**, *114*, 4424−4428.
(52) Merlen, A.; Bendiab, N.; Toulemonde, P.; Aouizerat, A.; San Miguel, A.; Sauvajol, J. L.; Montagnac, G.; Cardon, H.; Petit, P. Resonant Raman Spectroscopy of Single-Wall Carbon Nanotubes Under Pressure. *Phys. Rev. B* **2005**, *72*, 035409.